Weather and Climate Extremes 26 (2019) 100229

Contents lists available at ScienceDirect

Weather and Climate Extremes

journal homepage: http://www.elsevier.com/locate/wace

Physically-based landfalling tropical cyclone scenarios in support of risk assessment

Cindy L. Bruyère [a,b,*], James M. Done [a], Abigail B. Jaye [a], Greg J. Holland [a], Bruce Buckley [c], David J. Henderson [c], Mark Leplastrier [c], Peter Chan [c]

[a] National Center for Atmospheric Research (NCAR), 3090 Center Green Drive, Boulder, CO, 80301, USA
[b] Environmental Sciences and Management, North-West University, Potchefstroom, 2531, South Africa
[c] Insurance Australia Group Limited, Tower Two, Darling Park, 201 Sussex Street, Sydney, NSW, 2000, Australia

ARTICLE INFO

Keywords:
Tropical cyclones
WRF
Hybrid approach
Risk modeling

ABSTRACT

Populations and property values are increasing in tropical cyclone prone regions, driving up repair and replacement costs following a tropical cyclone impact. Climate change influences on tropical cyclones and sea levels will only exacerbate these rises. For example, Australia's Severe Tropical Cyclone Debbie in 2017 was one of the most destructive cyclones to make landfall in Australia since Tropical Cyclone Tracy in 1974. The primary impacts of Cyclone Debbie were due to extreme short duration intense wind driven rainfall and widespread major flooding, both linked to uncharacteristically warm sea surface temperatures. Studying the impact of climate change on tropical cyclones is limited by the lack of well observed historical events. Traditional hazard risk assessment approaches are limited since they are primarily based on statistical models which only deal with single meteorological hazards, or use simplified parameterized relationships when more than one phenomenon is included. Here we explore the value of dynamical models for creating targeted, detailed, and physically plausible multi-hazard tropical cyclone scenarios, through the development of a modeling system that i) retains a high degree of simulation control, ii) is globally applicable, and iii) is responsive to climate variability and change. Application of the modeling system to a thermodynamic climate change scenario finds that the tropical cyclone penetrates much further inland with a marked expansion of the heavy rainfall area, resulting in significantly larger areas subjected to damaging and destructive wind speeds and rainfall totals capable of producing flash and riverine flooding.

1. Introduction

As tropical cyclones (TCs) make landfall in increasingly populated regions, the costs rise (Weinkle et al., 2012). Trends in global losses indicate an approximate doubling of inflation-adjusted economic and insured losses every 15 years (Munich Re, 2018). While these increases have been driven primarily by increasing property values in TC-prone regions, changes to the TCs themselves (e.g., Holland and Bruyère, 2014) together with sea-level rise (Solomon, 2007; Nerem et al., 2018; Lin et al., 2012) has likely also contributed (Estrada et al., 2015). For example, the climate change contribution to rainfall totals from Hurricane Harvey was recently quantified at approximately an additional 40% (Risser and Wehner, 2017), and directly linked to warmer waters (Trenberth et al., 2018). Furthermore, Emanuel (2017) quantified a six-fold increase in the likelihood of Harvey's rainfall occurrence being due to climate change.

Cyclone Debbie (2017) was a recent example of a high rainfall cyclone connected to warmer than normal waters (SSTs close to or slightly above 30 °C: BoM, 2018a, 2018b). Debbie was one of the most destructive tropical cyclones to make landfall in Australia since cyclone Tracy in 1974. The primary impacts of the cyclone were due to extreme rainfall leading to flash and river flooding that extended hundreds of kilometers down the coast from the landfall point, and water ingress due to wind-driven rainfall. The town of Upper Springbrook received a record 890 mm of rain in 48 h, nearly equivalent to Brisbane's annual precipitation and 50% more than Melbourne's annual rainfall of 600 mm. The highest total precipitation (1307 mm) was recorded at Undercliff. Undercliff also reported the highest daily total for the event (544 mm). These precipitation amounts were well in excess of the 1% Annual Exceedance Probability (AEP - BoM, 2018a). Importantly, these

* Corresponding author. National Center for Atmospheric Research (NCAR), 3090 Center Green Drive, Boulder, CO, 80301, USA.
E-mail address: bruyerec@ucar.edu (C.L. Bruyère).

https://doi.org/10.1016/j.wace.2019.100229
Received 17 December 2018; Received in revised form 18 September 2019; Accepted 20 September 2019
Available online 22 September 2019

towns are located significantly south of the landfall location and well outside of the TC flood warning area as issued by the operational centers.

Further changes in TC related risks are likely (Walsh et al., 2016). Storm lifetime maximum wind speeds have migrated poleward over the past decades, and will continue to do so in a warming climate (Kossin et al., 2014), exposing new regions to TC impacts. Substantial future increases in TC rain rates within 100 km of the TC center are also expected (e.g., Christensen et al., 2013; Villarini et al., 2014). These changes could lead to more damaging events in the future (Morss et al., 2011) and the possibility of high-impact events outside the range of our experience that would render traditional risk assessment practices less effective (Milly et al., 2008). As TC exposure and potential damage increases, TC risk assessment needs to undergo a step change for society to properly confront this new era of TC risk (Cobb and Done, 2017).

TCs are complex multi-hazard phenomena, bringing concurrent extremes in wind, rainfall, wind-driven rainfall, severe thunderstorm outbreaks away from the cyclone center and storm surge. Hazard risk assessment therefore requires an understanding of these complex interactions. Moreover, using a single characteristic of a given variable may not capture all contributing damage processes. Take winds for example. While peak wind speeds are a primary driver of TC damage (Murnane and Elsner, 2012), wind duration, wind speeds at the times of peak rainfall intensities and the degree of wind directional change may also be important for weak to moderate TCs, and for the outer circulation of more intense cyclones (Done et al., 2018; Czajkowski and Done, 2014). Analyses of property damage during Australia's cyclones Marcia and Debbie revealed that 70 percent of claims included damage due to water ingress despite the fact that most of these properties did not sustain severe structural damage (CTS, 2018). Characterization of the full 4-dimensional wind field therefore becomes important for comprehensive multi-factor risk assessment. Further, freshwater flooding and attendant losses may extend far inland (Czajkowski et al., 2017) and storm surge exacts a heavy toll – both of these require good wind information.

Traditional hazard risk assessment is based primarily on statistical models (Lin et al., 2010). These statistical approaches have the advantage of efficiency that enables thousands of simulations. These models generate tens of thousands of synthetic events through repeated random sampling of local and regional historical TC parameters, such as track location, forward speed and heading, maximum wind speed and rate of change of wind speed (e.g., Hall and Sobel, 2013; Hall and Jewson, 2007; Rumpf et al., 2007; Vickery et al., 2000). But they are lacking in important ways for risk assessment. The models lack information on key damaging features such as accurate TC size, precipitation and eye-wall replacement cycles (Wakimoto and Black, 1994). Statistical models also may be susceptible to physical inconsistencies between variables and from the lack of spatial and temporal coherence of the damaging wind fields and intense rainfall, particularly over complex terrain. These methods also typically only deal with one meteorological hazard, or having simplified heavily parameterized relationships if more than one phenomenon is included. Spatial wind fields are assigned according to parametric wind field models (e.g., Holland et al., 2010; Willoughby et al., 2006), with TC size included to the extent that TC size is observed in the historical record. Storm surge is sometimes included using synthetic storm wind fields to drive a surge model (Lin et al., 2012). Rainfall is also sometimes included (e.g., Grieser and Jewson, 2012) using models based on historical rainfall statistics (Lonfat et al., 2007) or physical principles (Langousis and Veneziano, 2009).

With a warming climate, today's statistical modeling approaches do not adequately reflect the current risks posed by increased quantities of rainfall that produce damage from both wind-driven rainfall and flash flooding. The increasing intensity and spatial extent of the heavy rainfall in a warming climate is also inadequately included in traditional modeling approaches. Traditional statistical approaches, which are based on the observed historical record, are less likely to handle rare but extreme events well (Li et al., 2015) since they use climatological data that under-represents the near-recent and future risks. Finally, Lavender et al. (2018) cautioned against extrapolating results with average environmental temperature: Linear scaling relationships between extreme precipitation and temperature may not hold due to the compounding effect of intensifying TC circulations and convergence. These studies provide further motivation for a physically-based modeling system.

Dynamical models provide a wealth of information on key damaging parameters. Recent global models have been run using grid spacing of 10–25 km, at which many key damaging TC parameters start to become resolved (Bacmeister et al., 2018; Shaevitz et al., 2014). They have also been used to assess changes in TC rainfall (Villarini et al., 2014). Yet, they are primarily used to simulate observed events, they are prone to model biases, and are challenging to use in risk assessment (Cobb and Done, 2017). Perhaps the most severe limitation is the low sample size of dynamically modelled TCs compared to their statistical counterparts: the number of simulated years by global and regional climate models are typically limited to the low hundreds (Bruyère et al., 2017; Done et al., 2015). Yet exploratory work has demonstrated the use of dynamical models for TC risk assessment (Gettelman et al., 2018; Vitolo et al., 2010). In recognition of these limitations, more recent work has explored the value of combined statistical-dynamical approaches (e.g., Lee et al., 2018).

The historical Australian TC record has a relatively short period in which the tropical cyclone characteristics are well observed and the analyses considered to be reliable (BoM, 2018b). Despite this short reliable record, significant changes have been observed. The numbers of strong TCs have increased (Kuleshov et al., 2010; Holland and Bruyère, 2014) and the storm lifetime peak intensity has migrated southward (Kossin et al., 2014). Further changes are predicted for the region. Lavender and Walsh (2011) found additional southward migration of peak intensities, meaning that cities along the south eastern Queensland, north eastern NSW and south western Australian coasts will experience TCs more often than in the past. Extratropical transitioning cyclones are also extending their impacts to higher latitudes, increasing the risk for countries like New Zealand. Parker et al. (2018) found a 5–10% increases in Eastern Australian landfall wind speed and up to 27% increase in TC rain rates under an end-of-century RCP8.5 scenario. This makes Australia a good case-study region to develop a modeling system that has application to increasing the sample size.

Physically credible scenarios are key aids for risk management decisions (Loridan and Mason, 2017; Borio et al., 2014) and are commonly used to stress test current practices and adaptations. Developing new hybrid approaches, as described here, that apply dynamical modeling but use a more targeted simulation approach have the potential to add value to current risk assessment practices. One advantage of a hybrid approach is the generation of TC scenarios that fall outside distributions fitted to the historical record but are physically plausible. These new modeling approaches are not intended to replace statistical risk assessment methods, but rather they can be used to understand what statistical approaches may be missing. This is especially true in data-scarce regions, like Australia, and in adding climate change and variability components to traditional risk assessment methods. This study explores the value of dynamical models for creating targeted, detailed, and physically possible multi-hazard TC scenarios. We develop and demonstrate a modeling system that i) retains a high degree of simulation control, ii) is globally applicable, and iii) is responsive to climate variability and change. While the approach is globally applicable we develop and demonstrate the model for the case study region of the East Coast of Australia.

The next section describes the development and setup of the hybrid WRF cyclone model (HWCM). A series of model performance and sensitivity tests are established in sections 3 and 4. Section 5 presents results of a climate change study. The potential value of this approach for supporting risk management is discussed in Section 6, and

conclusions are presented in Section 7.

2. HWCM design and setup

Idealized numerical models are powerful tools to understand processes within a controlled and simplified system. They are not a new concept. To name but a few: Tuleya and Kurihara (1978) and Tuleya et al. (1984) developed an idealized movable mesh-model to investigate characteristics of landfalling cyclones. Kimball (2008) adapted a version of the Pennsylvania State University - National Center for Atmospheric Research (NCAR) Mesoscale Model (MM5) to study the evolution of rainfall in simulated landfalling cyclones, while Li et al. (2015) used the idealized component of the Weather Research and Forecasting model (WRF: Skamarock et al., 2008) to study the effects of land-sea contrasts on tropical cyclone precipitation. Although all of these studies contributed to our knowledge and understanding of landfalling cyclones, they all had similar limitations. They all used an *f*-plane and a flat land surface with straight coastlines, limiting application to real-world scenarios.

The development of the Hybrid WRF Cyclone Model (HWCM) makes use of both the real and idealized components of the WRF modeling system. This enables exploration of idealized physically-plausible multi-hazard TC scenarios that include the real-world complexities of a β-plane, real coastlines and topography. The HWCM makes use of a two-step process: 1) the idealized tropical cyclone component of WRF is used to establish a spun-up, realistic 3-dimensional tropical cyclone; and 2) this cyclone is placed in a synthetic real-world environment where its movement is constrained, but it is freely allowed to develop and interact with land.

2.1. Idealized configuration

The first step in setting up the HWCM model is to spin up a mature tropical cyclone in an idealized configuration (for details on the configuration of idealized cyclones in WRF, see Rotunno et al., 2009). The initial disturbance for all simulations (unless stated otherwise) is a synthetic tropical cyclone-like axisymmetric vortex (Fig. 1a) with 15 ms^{-1} maximum lowest-level winds. The initial cyclone size, e.g. the radius of maximum winds (RMW) is set to 82.5 km, and the radius of zero wind is 412.5 km. The vortex decays in the vertical with log-pressure. A spatially uniform Coriolis parameter is used, representative of 20°S, as southern hemisphere cyclones are being simulated. Typical sea surface temperatures (SSTs) for the Australian cyclone season are between 27 and 29 °C for the Queensland coast and adjacent Coral Sea, which is the focus of this study. For current climate simulations SST is fixed at 28 °C. A moist tropical atmosphere (Fig. 2 - after Dunion and Marron 2008; Dunion 2011) is used in the simulations, as it is the most supportive for cyclone formation and intensification.

The TC is then spun up in a 3000 × 3000 km domain with a horizontal grid spacing of 12 km, to match the grid spacing of the real-world environment simulations. Periodic boundaries are used, and therefore no boundary conditions are needed in this step. The cyclone was allowed to intensify until it reached a steady state (Fig. 3), which occurred after approximately two days, at which point the cyclone was a category 3 (Saffir-Simpson scale) storm. The resolution used here is somewhat coarser than what is needed to resolve the intensity of the most intense TCs (Davis, 2018), but was chosen to balance the need for sufficiently high resolution with the ability to generate a large number of test simulations. Practically, higher resolution will be needed when using the HWCM data as drivers for risk assessment.

2.2. Real configuration

Once the largely-symmetric mature TC (Fig. 1b) has been established, it is placed inside a real-world domain (Fig. 1c). The cyclone is placed far enough from land to ensure sufficient time to dynamically evolve before making landfall. The initial environmental conditions surrounding the cyclone are moist tropical (Fig. 2). The initial surface conditions over land are set to the climatological average for the cyclone season, while SST is time independent and spatially uniform (for more details see section 4a). Additionally, our real-world domain contains all the invariant data contained in regular WRF simulations, such as terrain and landmask.

Observed cyclone propagation (Holland, 1983) is prescribed by a nonlinear interaction between the earth's vorticity field and an atmospheric background flow. In our simulations cyclone propagation and steering is prescribed by the earth's vorticity field (model simulations are conducted on a β-plane) and a user defined environmental background wind flow (refer to Fig. 10) to move the cyclone along a prescribed track.

Over time, the cyclone and its environment are allowed to evolve dynamically, while zero tendencies (Skamarock et al., 2008) on the boundaries provide the constant environmental flow used for steering. The initial placement of the cyclone and the background wind flow allow some control over TC translation speed and landfall location and angle, while ensuring sufficient dynamical freedom for the TC to respond to forcing from land and topography.

All model simulations are performed on a 12-km horizontal grid over a domain covering Australia and a large section of the South West Pacific Ocean (Fig. 1c). The physical parameterization schemes used are a set typically used for TC simulations: RRTMG radiation (Mlawer et al. 1997); Tiedtke cumulus (Tiedtke 1989); WSM6 microphysics (Hong et al. 2004); YSU planetary boundary layer (Hong et al. 2006); and the Noah land surface scheme (Chen and Dudhia 2001). Parker et al. (2018) used a similar resolution and configuration for TC simulations over Australia and found that they produced realistic simulations.

Due to the fact that a well-developed TC is placed within a uniform background environment, an adjustment and further spin-up time is required. To lessen any initial shock a 2-h digital filter initialization[1] (Skamarock et al., 2008; Huang and Yang, 2002; Weygandt and Benjamin, 2007) is applied to all simulations, after which the first 12 h are used as an additional spin-up period.

3. Model performance with increasing model complexity

To test the stability and robustness of the HWCM a series of sensitivity tests were performed: an aqua-planet (AP) simulation spun up from a uniform background and allowed to evolve (AP1); same as AP1 but with a cyclone inserted into the background at the start of the simulation (AP2); a real-world (RW) simulation containing land, but the background environment was uniform at the initial time (RW1); and, same as RW1 but with a cyclone (same cyclone as in AP2) inserted (RW2). Figs. 4 and 5 show snapshots of the environments in these sensitivity runs just prior to landfall and just before the end of the simulations, respectively. AP1 and AP2 do not contain land, but the Australian coast is plotted for reference. Nominal landfall in all simulations is denoted as the landfall time that corresponds to that observed in RW2.

AP1 establishes a subtropical high-pressure system, as can be expected for an aqua-planet simulation (Sumi, 1992). With zero tendencies on the boundaries the evolution of weather systems is driven by latitudinal variations in Coriolis, absorption of solar radiation, and the diurnal cycle. The major difference between the first and second snapshots (Figs. 4a and 5a) is that the second *(night time)* is somewhat colder than the first *(early morning)*. Embedding a cyclone into this simulation (AP2: Figs. 4b and 5b) results in the weather systems evolving to accommodate its presence. RW1, initialized with a uniform background

[1] DFI is a technique whereby a digital filter is applied during a short forward/backward model integration before the forecast is started. This initialization technique is used to remove any initial model imbalances.

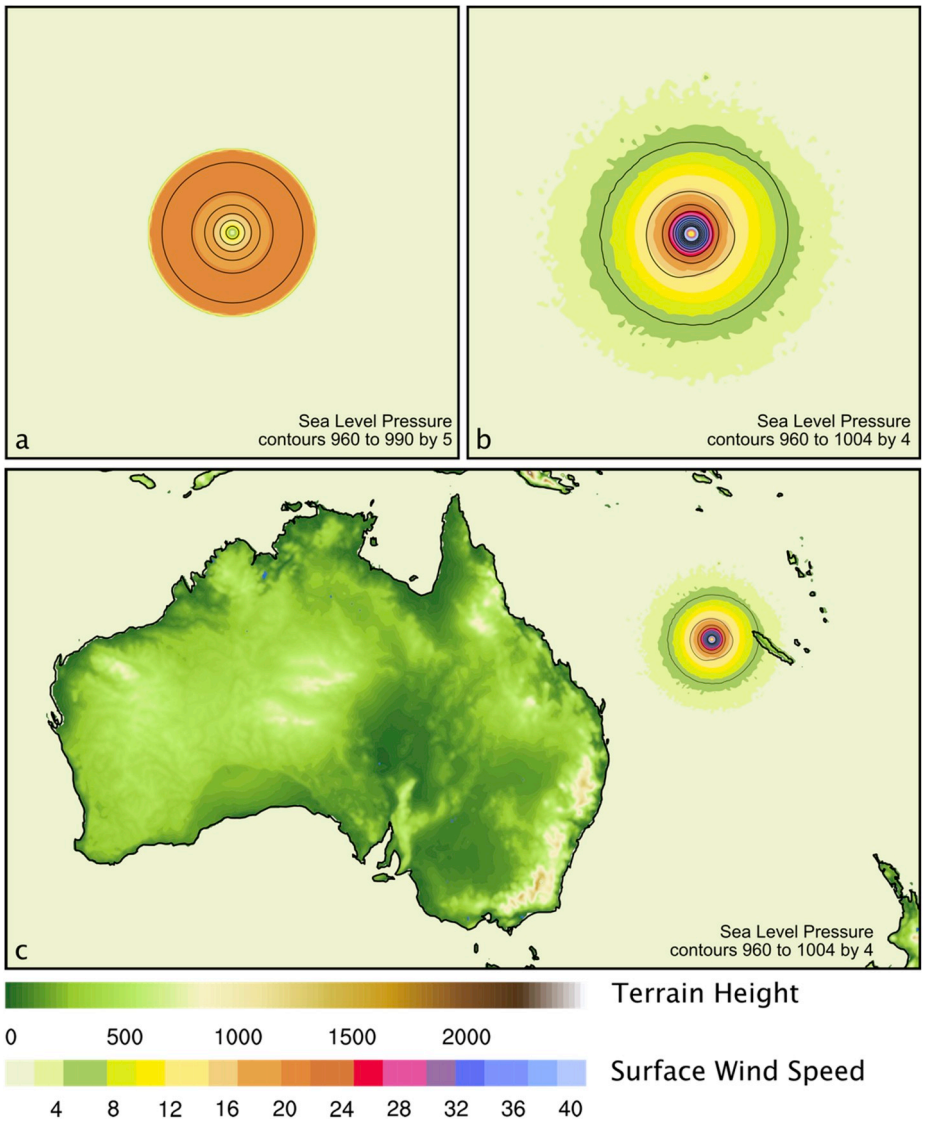

Fig. 1. Idealized tropical cyclone as a weak initial vortex (a), and a well spun-up category 3 cyclone (b). Bottom figure (c) depicts the mature cyclone placed in a real-world domain. Colors indicate wind speed (m/s) and contours surface pressure (hPa). Color over land is terrain height (m) as used in the real-world simulations. (For interpretation of the references to colour in this figure legend, the reader is referred to the Web version of this article.)

in a real-world domain, shows similar environmental features being established as in AP1, but with some flow modification due to the presence of land and topography. And finally, as for simulation AP2, the introduction of a cyclone in RW2 results in similar environmental conditions as for RW1, but with the environmental conditions now incorporating this system.

Before examining the effect of other environmental factors on cyclone behavior, we evaluate the effect of land. Fig. 6 shows the cyclone maximum surface wind, minimum pressure and translation speed for AP2 and RW2. For RW2 the cyclone made landfall after a little more than 2 days simulation (hour 56), the time used as the nominal landfall point for both simulations. During the first few hours of the simulations the cyclones in both cases developed similarly. Approximately 30 h after initialization, and about a day before nominal landfall, RW2 weakened slightly as it started to interact with land. After landfall the cyclone rapidly weakened to below 17 m/s (model wind speeds are at 10 m above the surface and approximate the 1-min sustained values). AP2, on the other hand, remained at TC strength for nearly four days and only started to weaken as it moved to higher latitudes. Similarly, the translation speed of RW2 started to oscillate as it moved over land, likely due to the interaction with varying topography, while AP2's translation speed increased as it moved to higher latitudes.

The next section examines simulation sensitivity to other environmental factors, specifically changes in SST forcing, changes in background flow, intensity and cyclone size.

4. Sensitivity testing

The initial conditions for the simulations used in this section are summarized in Table 1.

4.1. Effect of SST

Cyclones commonly travel over varying SSTs, and are affected by both the absolute value (Palmén, 1948; Gray, 1968) and the gradient (Lindzen and Nigam, 1987) of change that they encounter. Lindzen and Nigam (1987) suggested that thermally induced pressure gradients across SST values can accelerate flow from colder regions to warmer regions. As SSTs increase/decrease, TCs can also gain/lose intensity, which can affect translation speed and direction. For the hybrid simulations, this adds an additional level of uncertainty that makes it harder to 1) control the path a cyclone will take, and 2) attribute differences

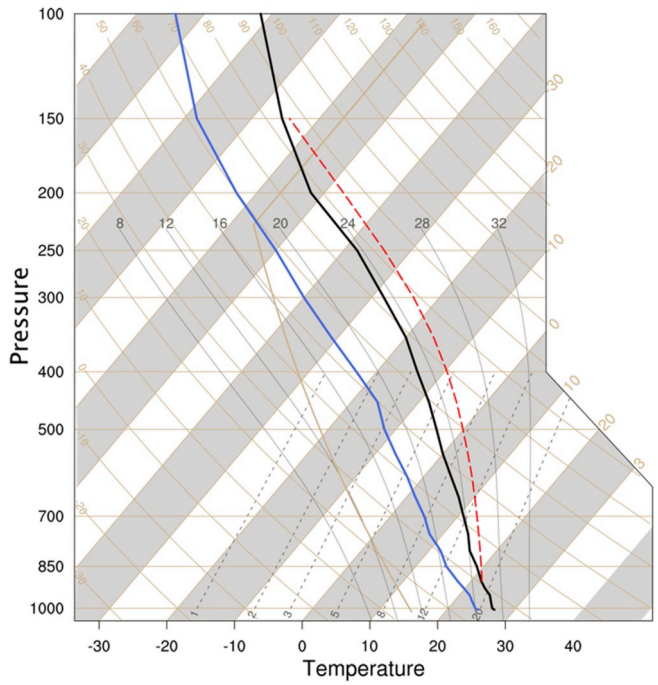

Fig. 2. Upper-air sounding for an average Tropical Cyclone environment (after Dunion and Marron 2008; Dunion 2011). The units of temperature and pressure are °C and hPa, respectively.

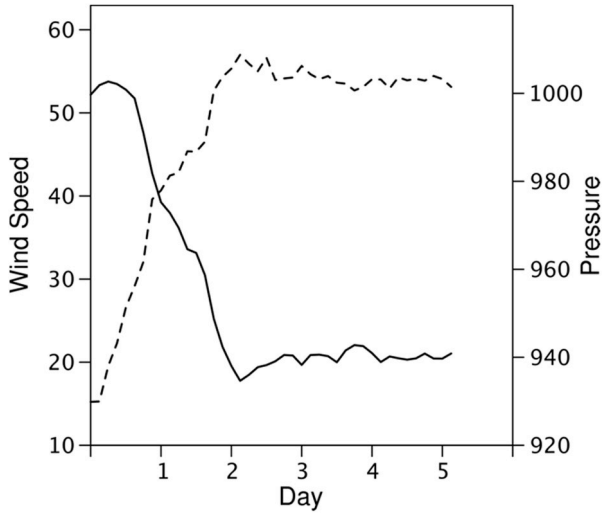

Fig. 3. Time series of maximum sustained wind speed (m/s – dash line) and minimum central pressure (hPa – solid line) development of the idealized cyclone.

between simulations to a single process. The solution to these complications is to use a constant SST (Tuleya and Kurihara, 1978; Tuleya et al., 1984; Kimball, 2008; Li et al., 2015) for the hybrid simulations. But first we need to establish the impact this has on the simulations.

To evaluate the effect of SST on cyclone development and movement, two simulations were performed. In the first (SST_C) the SST for the entire domain was set to a constant value of 28 °C, while a varying SST (Fig. 7) was used for the second (SST_V). The varying SST was constructed using the 1990–2000 February (the midpoint in the South Pacific cyclone season) average SST. *The digital filter initialization technique and a long spin-up period is used to remove the initial imbalance between the large-scale atmosphere and SSTs.* For both simulations the initial cyclone was placed well off-shore and the prescribed background wind flow was set to ensure that the cyclone remains over water. For the simulation with varying SST, the cyclone encounters steep SST gradients (see Fig. 8a for the SST change during the simulation).

Initially, both cyclones develop very similarly, as can be seen in the wind and pressure plot (Fig. 8c). The total precipitation in a 500 km radius around the cyclone center also is initially similar for both cyclones (Fig. 8b). As the cyclones develop, the cyclone over the varying SST field becomes weaker and produces less precipitation than the TC over constant SST. In summary, the effect of using a constant SST is to maintain the TC strength as it propagates poleward. As using a constant SST does not negatively affect the cyclone development, and has the added benefit of simplifying the comparison of simulations, all other simulations use a constant SST value.

4.2. *Effect of the steering flow*

As for the SST sensitivity case, in a real-world environment TCs experience vastly different steering flows, which is a major reason why it is difficult to quantitatively compare two different cyclones. A main motivation for the development of the HWCM is the ability to control the steering flow, and thus the track. In order to test the cyclone sensitivity to the background flow two pairs of experiments were conducted: 1) the strength of the background steering flow was altered; and 2) the 850-200 hPa vertical shear was altered.

In the background flow experiment (1), the cyclone was subjected to either a vertically constant 10 knot (~5 m/s) or 20 knot (~10 m/s) steering flow (Table 1: SF10 and SF20). Both cyclones developed very similarly for the first 80 h, as can be seen from the wind and pressure plot (Fig. 9b). The change only impacted the translation speed of the cyclones, with the one placed in the stronger flow traveling a total distance of 900 nautical miles over 5 days, compared to 600 nautical miles for the cyclone experiencing the weaker background flow. This increased translation speed resulted in an earlier landfalling time (80 h into the simulation), after which the faster moving cyclone rapidly dissipated over land while the slower cyclone remained over water and therefore maintained intensity.

Of all environmental conditions, strong vertical wind shear can be one of the most inhibiting for cyclone genesis and intensification (DeMaria and Kaplan, 1994; Kaplan and DeMaria, 2003; Emanuel et al., 2004). This applies particularly to very-high vertical shear. Under some environmental conditions, weak to moderate shear can be beneficial to cyclone development. Onderlinde and Nolan (2014) showed that for positive storm relative helicity cyclones develop and intensify faster, while Finocchio et al. (2016) found that weak to moderate upper atmosphere shear promotes intensification.

To test the impact of shear (experiment 2), 4 sensitivity simulations were conducted by altering the vertical shear from zero (SH00) to weak (5 and 7 m/s; SH05 and SH07), and to moderate (10 m/s; SH10) (Fig. 10). Positive relative helicity and upper-air shear was used. The introduction of vertical shear changes the upper level cyclone ventilation (Tang and Emanuel, 2012). Therefore, regardless of the strength of the shear, all the shear runs differ more from the zero-shear simulation than from one another. The biggest impacts due to the introduction of shear are on precipitation and the spatial distribution of surface winds. The lifetime precipitation in a 500 km area around the center of the cyclone is about 16% higher for all the shear cases compared to the zero-shear case (Fig. 11). In all four simulations the peak cyclone intensities are nearly identical (last row in Table 2). However, a weak to moderate upper-air shear environment expands the area of strong surface winds (Table 2). For instance, in a 5 m/s shear environment, the area impacted by category 1/2 (Saffir-Simpson) winds increases by 28/50% compared to a zero-shear environment. This expansion of surface wind distribution to higher intensities is slightly less for the moderate shear environment than the weaker shear cases.

The shear simulations also have slightly higher translation speeds. When shear is introduced the cyclones travel between 15 and 20%

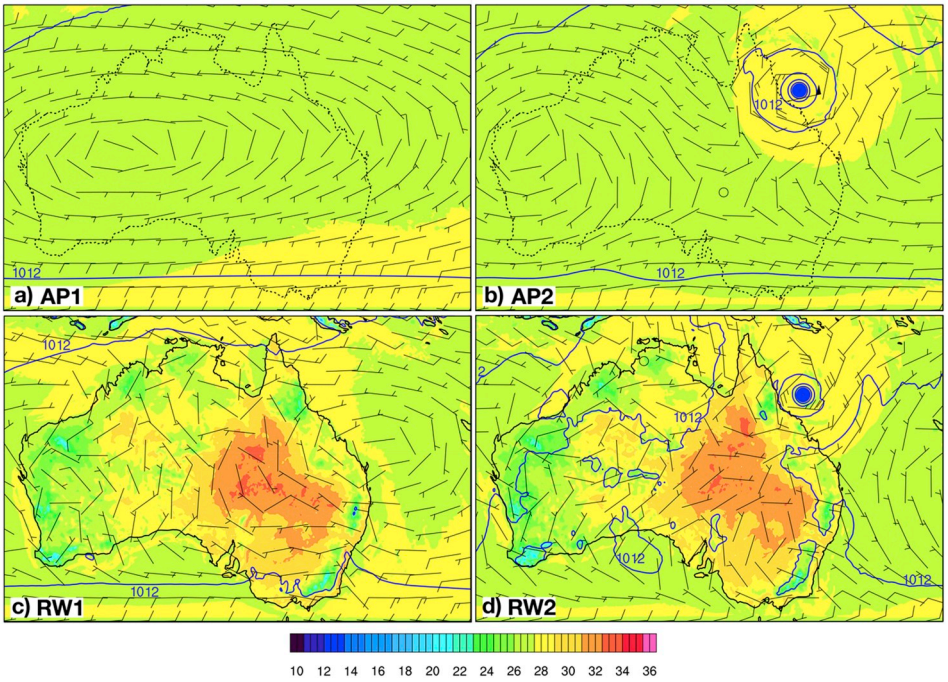

Fig. 4. Sensitivity experiments for the aqua-planet (a and b) and real-world (c and d) simulations with (b and d) and without (a and c) an embedded cyclone at the time of nominal land-fall. Colors represents surface temperature (°C) and surface winds are plotted as wind barbs (m/s). AP1 and AP2 do not contain land, but the Australian coast is plotted as a dotted outline for reference. (For interpretation of the references to colour in this figure legend, the reader is referred to the Web version of this article.)

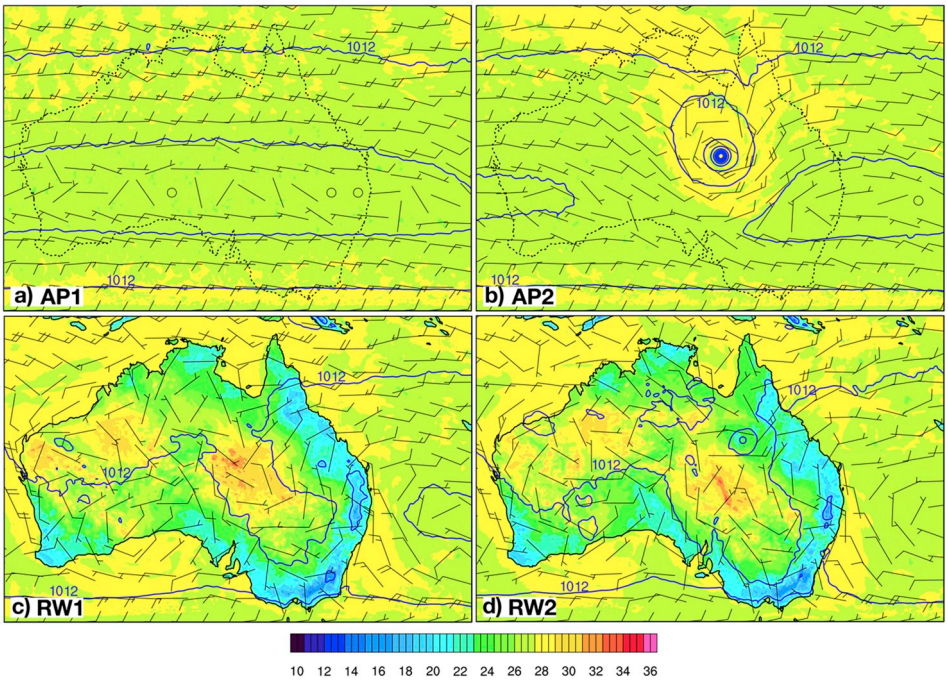

Fig. 5. Same as Fig. 4, but for a time close to the end of the simulation.

further than the control case with zero shear.

As a constant wind profile is not realistic, all remaining simulations were performed with moderate vertical shear.

4.3. Effect of initial cyclone size and intensity

The final set of sensitivity tests perturb the initial vortices while keeping the background conditions constant (i.e., initial conditions set to a moist tropical atmosphere, steering flow with moderate upper-level shear, and a constant SST of 28 °C). The aim of these experiments is to understand the impact of the initial disturbance relative to the environment they experience during their lifetime. For these experiments either the initial radius of maximum winds (cyclone size) or the initial cyclone intensity are perturbed from those described in section 2a. The size experiments use vortices with RMW's one-third and two-thirds smaller (i.e., 55 and 30 km, respectively), while the intensity experiments are 15 and 30% stronger (17 and 20 m/s, respectively). The control case is denoted S82_I15, while the size experiments are SIZE55 and SIZE30, and the intensity experiments INT17 and INT20 (Table 1). The difference in initial sizes is eliminated rapidly after the cyclones are placed in the same environment. Over the lifetime of the cyclones, the smaller size cyclones are slightly less intense compared to the control

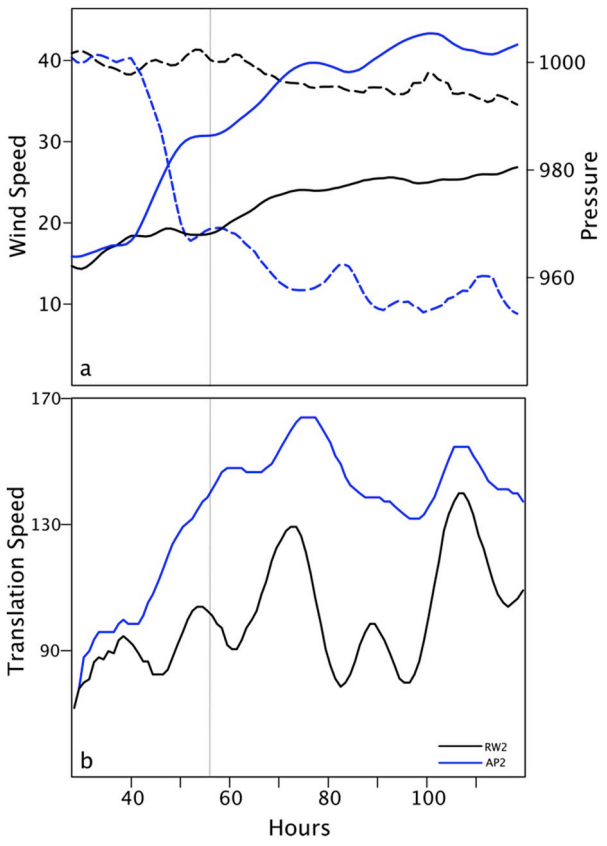

Fig. 6. Maximum sustained wind speed (m/s – dash line) and minimum central pressure (hPa – solid line) (a); and translation speed (nm/6 h) (b) for AP2 (blue) and RW2 (black). The fine grey line indicates the nominal time of landfall. (For interpretation of the references to colour in this figure legend, the reader is referred to the Web version of this article.)

and they produce slightly less precipitation (Fig. 12, blue lines). The more intense initial vortices follow a similar pattern with only the most intense initial cyclone maintaining a higher intensity over its lifetime. The higher initial intensity cyclones produce higher lifetime precipitation totals (Fig. 12, red lines). None of these differences are substantial, pointing to the environment being more important to cyclone development than the initial vortex size and intensity.

5. Impact of climate change

The link between SST and tropical cyclones is well established (Palmén, 1948; Gray, 1968; Anthes, 1982). Emanuel (1986) emphasized that surface fluxes ultimately determined the thermal structure of the mature tropical cyclone and therefore its intensity. Merrill (1988) quantified this with his "empirical potential intensity" relationship between SST and intensity. Here we examine the potential for climate change to modulate cyclone characteristics such as intensity, size, translation speed and precipitation.

Looking to the future, the dominant effect of increasing greenhouse gases on tropical cyclones is through the increasing upper ocean temperatures (Zhao et al., 2013; Knutson et al., 2010, 2015; Walsh et al.,

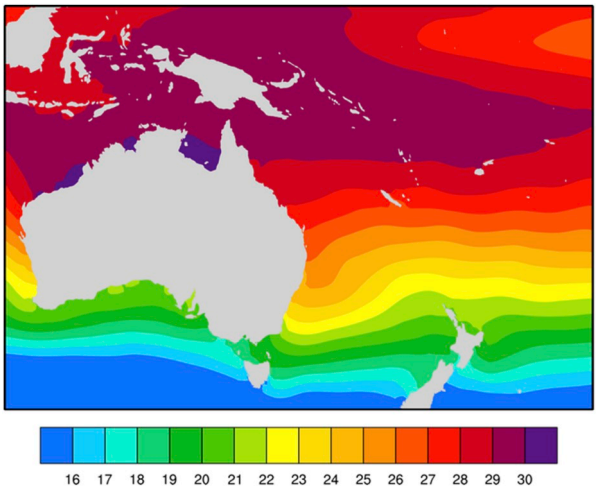

Fig. 7. Climatological sea surface temperature (°C) for the South West Pacific basin for the month of February for the period 1990–2000.

Table 1
Difference in the sensitivity experiments. AP1 and AP2 are the only simulations performed without real land and topography. AP1 and RW1 were the only simulation performed without an embedded cyclone. Comparison simulations are grouped together and difference between simulations are highlighted in bold. *SH10, S82_I15 and Current Climate are the same simulation, just renamed for ease of comparisons.

	SST (°C)	STEERING (M/S)	INITIAL SIZE (KM)	INITIAL INTENSITY (M/S)	CAPE (J/KG)
AP1	28	constant 5	82	15	1870
AP2	28	constant 5	82	15	1870
RW2	28	constant 5	82	15	1870
RW2	28	constant 5	82	15	1870
SST_C	**28**	constant 5	82	15	1870
SST_V	**climate**	constant 5	82	15	1870
SF10	28	**constant 5**	82	15	1870
SF20	28	**constant 10**	82	15	1870
SH00	28	**constant 5**	82	15	1870
SH05	28	**shear 5**	82	15	1870
SH07	28	**shear 7**	82	15	1870
SH10*	28	**shear 10**	82	15	1870
S82_I15*	28	shear 10	82	15	1870
SIZE55	28	shear 10	**55**	15	1870
SIZE30	28	shear 10	**30**	15	1870
INT17	28	shear 10	82	**17**	1870
INT20	28	shear 10	82	**20**	1870
PRE-INDUSTRIAL	**27**	shear 10	82	15	**1450**
CURRENT CLIMATE*	**28**	shear 10	82	15	**1870**
FUTURE CLIMATE	**31**	shear 10	82	15	**2418**

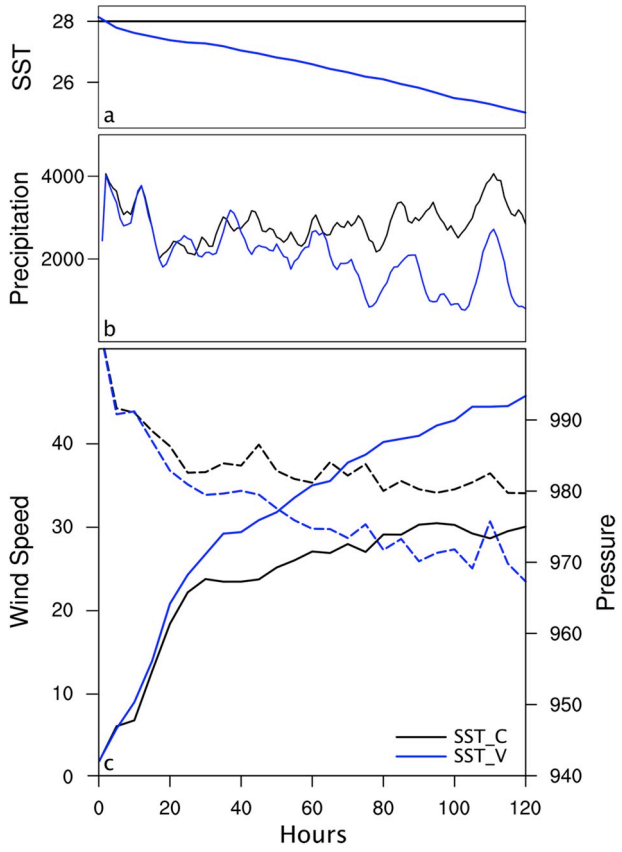

Fig. 8. SST change (°C) throughout the life cycle of TCs (a); Hourly integrated precipitation (mm/h) in a 500 km radius around the cyclone centers (b); and the cyclone maximum sustained wind (m/s – dash line) and minimum central pressure (hPa – solid line) changes (c) for the SST sensitivity test. Black lines are for the control case using a constant SST value of 28 °C (SST_C), while the blue lines are for the case using a climatological SST field (SST_V). (For interpretation of the references to colour in this figure legend, the reader is referred to the Web version of this article.)

2016). Christensen et al. (2013) concluded that the likely effects of this increase are to boost wind speeds and TC rain rate. Lighthill et al. (1993) and Henderson-Sellers et al. (1998) suggested that the maximum lifetime intensity would increase by 5–10% per ^{o}C of oceanic warming. Knutson et al. (1998) simulated western Pacific storms under current and future climate conditions and found that an increase of roughly 2.2 °C in SSTs resulted in cyclone intensities increasing by up to 7 m/s.

Gutmann et al. (2018) used high resolution WRF simulations and concluded that future cyclones will be more intense and have higher precipitation rates. They noted a statistically significant increase in occurrences of TC precipitation rates greater than 100 mm/h. Emanuel (2017) evaluated Hurricane Harvey's rainfall in current and future climate scenarios and estimated that what was a once in a 2,000-y event for the late 20th century, will become a once in a 100-y event by the end of the 21st century. Trenberth et al. (2018) also found that the rainfall for Harvey came from evaporation out of the nearby, anomalously-warm ocean temperatures.

Here we investigate the impact of pre-industrial, and future climate conditions on characteristics of a TC generated using HWCM, specifically intensity and precipitation. Note, we are not considering whether cyclones will develop or not under climate change conditions. Here we are investigating how characteristics of the TC differs under these altered thermodynamic conditions, given a cyclone in the same location. To achieve this, the SST and moist tropical temperature and moisture profile in Fig. 2 are perturbed to represent average conditions from pre-industrial and end of 21st century climate. The pre-industrial and future

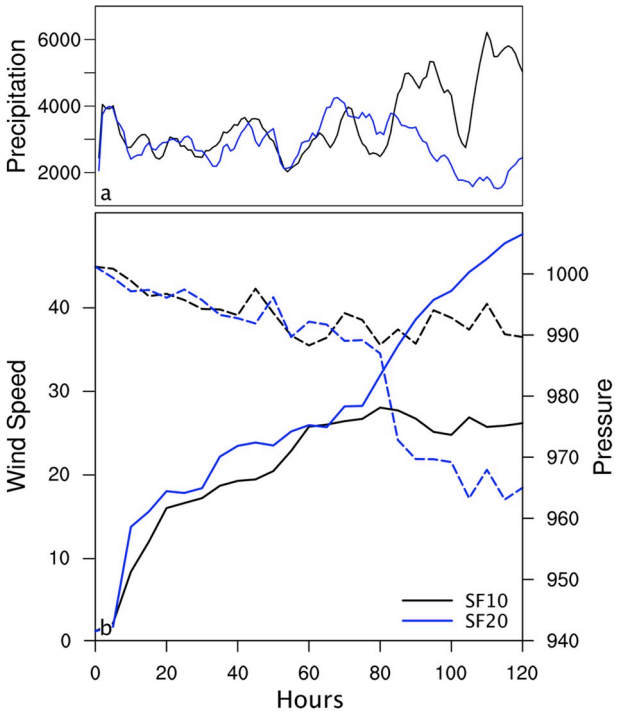

Fig. 9. Hourly integrated precipitation (mm/h) in a 500 km radius around the cyclone center (a); and the cyclone maximum sustained wind (m/s – dash line) and minimum central pressure changes (hPa – solid line) (b) for the altered background steering flow sensitivity test. Black lines are for the case with a weaker (5 m/s – SF10) background flow and blue for the stronger (10 m/s – SF20) background flow. (For interpretation of the references to colour in this figure legend, the reader is referred to the Web version of this article.)

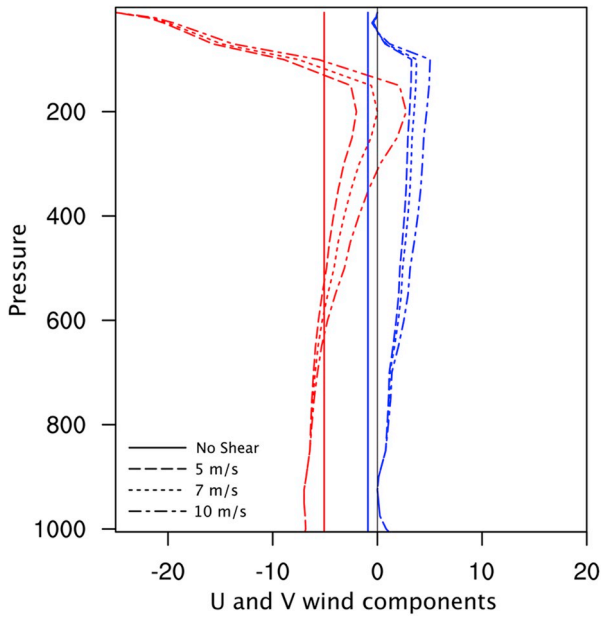

Fig. 10. Vertical wind profiles used in the simulations. The profiles used varied between no vertical shear and 10 m/s shear as indicated by the dashed lines. Red/blue lines represents the U and V components of the wind, respectively. (For interpretation of the references to colour in this figure legend, the reader is referred to the Web version of this article.)

SST and profiles were constructed using a 10-year average of the Australian cyclone season environment from the CESM pre-industrial and RCP8.5 end of century simulations (http://www.cesm.ucar.edu/e

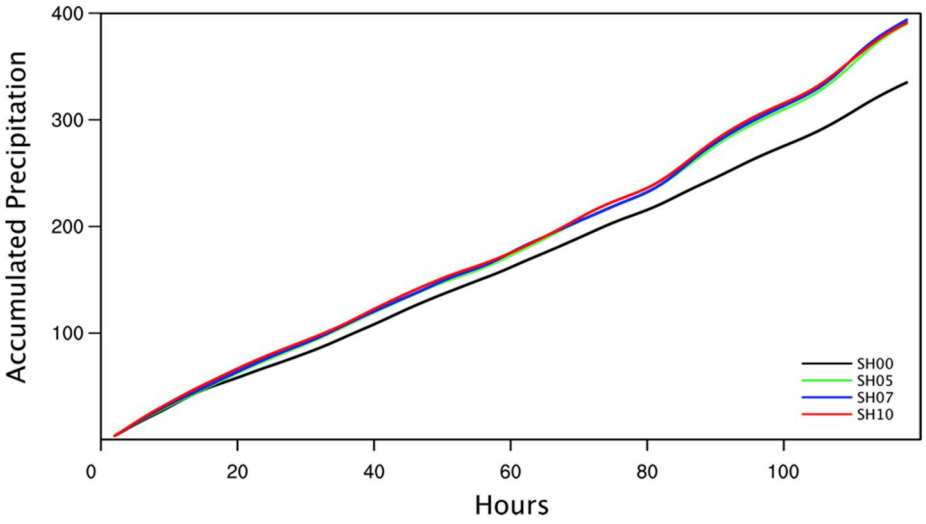

Fig. 11. Hourly accumulated precipitation (1000 mm/h) in a 500 km radius around the cyclone center for simulations with varying magnitudes of upper level shear.

Table 2
Percent increase in the total area exceeding TD, Cat 1, and Cat 2 intensities (Saffir-Simpson) between the zero shear and the 5, 7 and 10 m/s shear simulations, as well as the percent difference in storm lifetime maximum intensity.

	5 M/S	7 M/S	10 M/S
Tropical depression	28.3	26.6	22.9
TC CAT 1	28.6	24.1	16.9
TC CAT 2	50.0	39.1	28.3
Max intensity	2.7	4.1	3.7

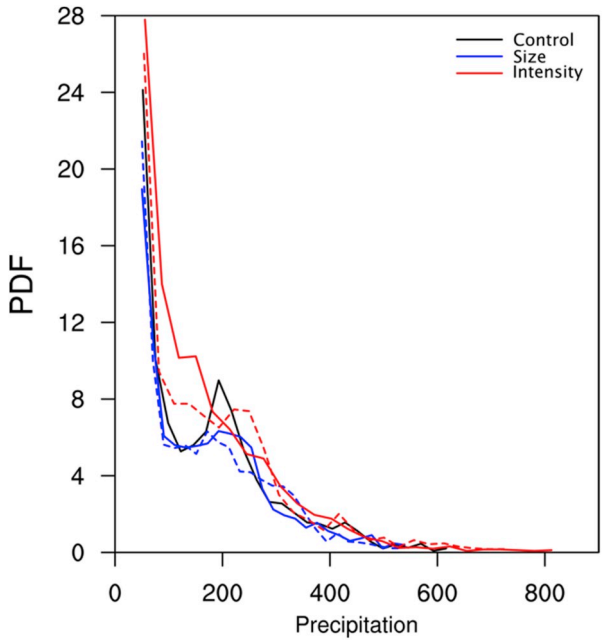

Fig. 12. Probability density function (PDF %) of the cyclone lifetime precipitation (mm). Black is the control case, while blue depicts the simulations with smaller initial size (solid/dash represents 55/33 km, respectively), and red depicts the simulations with higher initial intensity (solid/dash represents 20/17 m/s). (For interpretation of the references to colour in this figure legend, the reader is referred to the Web version of this article.)

xperiments/cesm1.0/). The average SST and atmospheric stability used for these runs are shown in the last three lines of Table 1. Using these new profiles, the same two-step process as described in section 2 is followed to (1) establish an initial cyclone and (2) simulate the cyclone development in a real-world environment.

The simulations were all run for 10 days, and the cyclones tracked until the central pressure increased to within 5 hPa of the average environmental pressure. Both the current and pre-industrial climate cyclones satisfied this pressure criteria for 6 days, and made landfall around day 4. The future-climate scenario cyclone had a faster translation speed, making landfall at day 3 and satisfied the pressure criteria for a total of 7.5 days, resulting in a total distance travelled of almost 70% farther than either the pre-industrial or current climate scenario cyclones.

Comparing the precipitation and wind footprints of the cyclones (Fig. 13), it is clear that both the precipitation intensity and maximum wind speed increases from the pre-industrial to the future scenario simulations. Before landfall the sustained wind speeds are tropical depression (TD)/category 1 and category 2 (Saffir-Simpson scale) for the pre-industrial/current and future climate scenario simulations. After landfall, both the current and pre-industrial scenario simulation cyclones dissipate quickly with only a small footprint of winds above TD strength. The future climate scenario cyclone makes landfall at category 2 and maintains higher speeds much further inland. The total rain volume (storm life-time total) within a 500 km radius around the cyclone center are −36/+120% (pre-industrial/future) compared to the precipitation volume for the current climate scenario, while the maximum rainfall rates are −23/+121% compared to the current climate scenario.

Differences over land are potentially the most significant from an impacts perspective. The future climate scenario cyclone penetrates much further inland resulting in significantly larger areas subjected to higher wind speeds and precipitation than either the pre-industrial or current climate scenario cyclones (Fig. 14). The sustained simulated inland wind speed increased from TD to category 1 strength. More significantly is the inland area that is subjected to wind speeds above 17 m/s increased by 500%. The maximum hourly precipitation over land is 45% higher than for the current climate, and the area with >50 mm in accumulated precipitation increased by 322%, and the total inland precipitation volume increased by 270%.

6. Potential value for risk management

Even the most recent comprehensive reanalysis products only apply to tropical cyclones since the 1980s, a length of record too short to

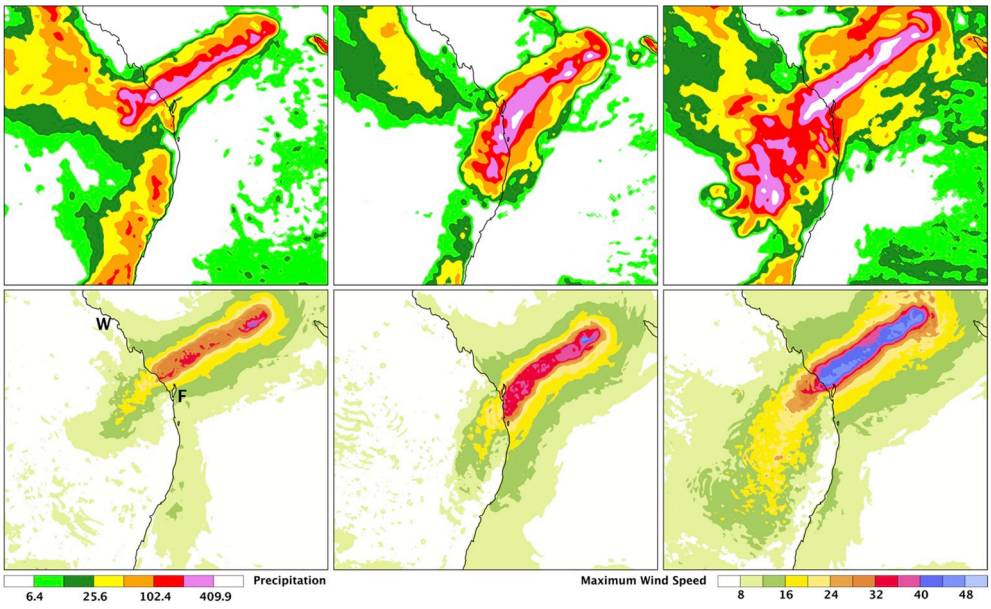

Fig. 13. Accumulated precipitation (mm) (top) and maximum wind speed footprint (m/s) (bottom) for the pre-industrial, current and future climate simulations. Fraser Island (F) and Whitsunday Region (W) are indicated on the lower left panel.

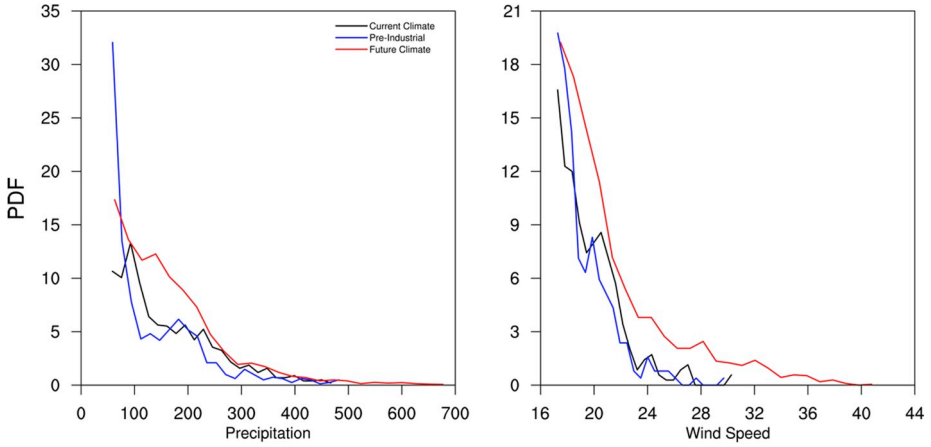

Fig. 14. Probability density function (PDF %) for the total lifetime precipitation volume in a 500 km radius around the cyclone (mm) (a); and storm lifetime maximum wind speed (m/s) over land (b) for the pre-industrial (blue), current (black) and future climate (red) simulations. (For interpretation of the references to colour in this figure legend, the reader is referred to the Web version of this article.)

adequately seed the statistically based cyclone risk models typically used for insurance and reinsurance purposes. Three areas of potential value of the HWCM for risk management are discussed here that derive from i) physically consistent views of multi-hazard TC events, ii) user-controlled simulation of events under current climate conditions, and iii) the ability to generate events under past and future climate conditions.

Currently, typical building codes have simplified design criteria (standards) to mitigate damage, all of which are focused on safety (e.g. maximum design wind speed to ensure a building does not structurally collapse during the passage of a design strength tropical cyclone, or 1% AEP flood impacts, both treated as independent events, which is not the case in the real world). The main design criteria for building in tropical cyclone regions focuses on wind loads (for instance, the Australian Wind Loading Standards - ASNZS1170.2). The supporting extreme wind analyses generally utilize the historical TC record with simplified TC structures, or extreme value analyses of very limited historical anemometer data, as many anemometers are damaged or destroyed well before peak winds speed are reached. Extensive tropical cyclone damage occurs from the coincidence of destructive wind speeds and heavy rainfall rates. The combined wind-rain effects produce significant damage to commercial buildings and domestic housing, but building codes do not make allowances for damages due to wind driven rainfall. Post-storm investigations conducted in Australia and internationally (Henderson and Ginger, 2008; Franco et al., 2010; Gurley and Masters, 2011; Boughton et al., 2017) have found that water ingress is a critical issue that requires extensive interior restoration. The main contributor to interior damage is wind-driven rain, which generate substantial damage at wind speeds well below contemporary design loads. Current wind engineering analyses may not adequately address risks associated with the increasing effects of greater quantities of wind driven rainfall entering buildings. Most tropical cyclone risk models used in the insurance and reinsurance industry also treat the risks posed by the wind fields and rainfall/flooding and storm surge as separate risks or as simplified risks that are heavily parameterized. Tropical cyclones generated using the HWCM approach produce tropical cyclone wind fields and rain fields and, when coupled to a surge model, could also generate storm surge extents. HWCM may therefore be used to increase

the sample size of events used by current risk assessment models, and to validate, calibrate and stress test current statistical methods.

HWCM simulated tropical cyclones can also be run at very high resolutions (eg., Rotunno et al., 2009) to better represent the interactions of the cyclone wind and rain fields with topography, a feature not adequately handled by statistical models alone. Structural engineering wind load design standards provide local site-specific topographic adjustment factors but these do not cater for changes in the wind structures of tropical cyclones due to the interaction of the tropical cyclone wind fields with larger topographical features such as the Australia's Great Dividing Range or the localized wind and rainfall patterns produced by complex topography. These topographical features also feed back on the TC structure and effect rainfall distributions and inland decay rates. Current risk assessment approaches traditionally adopt simple decay rate functions (e.g. Vickery, 2005) or other functions derived by historical events often based on the HURDAT (Landsea and Franklin, 2013) records, and used with a time over land decay rate. This technique does not account for the differing decay rates, the angle of approach of the tropical cyclone and its physical size. The simulations in this manuscript used a relatively low resolution, but as the HWCM can be run at different resolutions, land falling tropical cyclone impacts can be tuned to the complexity of the topography that surrounds the most vulnerable communities. The HWCM's ability to control cyclone paths and translation speeds by altering intensity and the background steering flow allows the creation of multiple impact scenarios with differing approach angles, translational speeds and intensities to better define the multi-parameter risks faced by vulnerable communities. These risks can include not only the potential for damage produced by destructive wind gusts but also the wind-driven rainfall, flash flooding, river flooding and, for coastal locations, storm surge.

Current generation tropical cyclone risk models used in the reinsurance and insurance industries do not adequately account for future changes in tropical cyclone risk (Milly et al., 2008; Lin et al. 2010; Cobb and Done, 2017). The historical tropical cyclone climate upon which the common wind engineering design criteria are based do not necessarily characterize the risks communities are facing as climate change effects increase. As the historical records have inherent limitations in accuracy and completeness (BoM, 2018b), this leads to uncertainties in reflecting the current and future climate that occurs within the design life of an asset. The typical design life of most new domestic structures is from 50 to 100 years, meaning they should cater for not only past but future climate tropical cyclone impacts. The HWCM approach informs the assessment of past, present and future climate tropical cyclone impacts, thus extending the amount of data for risk assessment purposes per scenario. This would enable risk managers to factor in the potential impacts of various climate change scenarios into the risk assessment process.

The feasibility of the HWCM model for risk assessments is exemplified by the similarities between the simulations in section 5 and the compound wind and rain impacts of Severe Tropical Cyclone Debbie. Of special note is the way that the heavy rainfall in this experiment extends well poleward of the landfall point, in the zone of onshore flow. Although these simulations were not reconstructions of TC Debbie, the extension of the rainfall patterns in the future climate simulation resembles the observed rainfall from Severe Tropical Cyclone Debbie (2017, see BoM, 2018a). In this case the idealized cyclone struck the east coast of Australia in the vicinity of Fraser Island (Fig. 13 lower left panel), the climate change scenario wind footprint and rainfall distribution in Fig. 13 bears striking similarities to that of Debbie that struck the Whitsunday region (Fig. 13 lower left panel), then recurved to the south and produced record rainfall across parts of southeast Queensland and the far northeast of New South Wales (NSW). And Debbie made landfall in an anomalously warm oceanic area of close to or slightly above 30 °C, similar to the SST used in the future climate simulations.

The HWCM model can assist emergency managers and insurance companies to stress test their portfolios to model more realistic and physically plausible extreme events (Lin and Emanuel 2016) that may not be self-evident from the limited historical tropical cyclone record of a past climate or whose impacts may not be adequately portrayed in simplified wind and rainfall models. In this way the risks faced by communities can be assessed with greater confidence, leading to the development of improved risk management strategies and ultimately allowing building codes and practices to be refined to consider regional variations in risk produced by topography and the potential impacts of climate change.

7. Conclusions

This study explored the value of dynamical models for creating targeted, detailed, and physically credible multi-hazard TC scenarios. Specifically, the Hybrid WRF Cyclone Model (HWCM) modeling system was developed to utilize both real and idealized components in the well-established WRF modeling system. This enables the generation of user-defined multi-hazard TC scenarios that account for the complexities of real-world coastlines, topography and both current and future climate scenarios.

A series of sensitivity studies tested the stability and robustness of the HWCM, before demonstrating an application for a climate change assessment over eastern Australia. The adequacy of the regional model domain was first established through a hierarchy of simulations of increasing model complexity, from aqua-planet to a TC interacting with real-world coastlines. A domain-wide constant SST was chosen to aid the interpretation. Changing the steering flow was shown to allow for a good degree of control on TC motion, thus enabling pre-determined tracks and cyclone characteristics to be assessed. Further testing using various vertical wind shear environments clearly showed the benefits of including a modest level of vertical wind shear in the simulations.

The resulting HWCM was applied to generate an example set of landfalling TC scenarios for Australia under large-scale environments representing pre-industrial, current, and future climate. This application explores the effect of thermodynamic change on TC behavior and does not consider climate change effects on TC occurrence. The resulting increases in TC peak wind speeds and overall rain rates were consistent with previous work. The future climate scenario showed substantial expansion of the areas impacted by damaging winds and high rainfall. For example, the future climate scenario generated a three-fold increase in land area experiencing high rainfall and a five-fold increase in land area experiencing high winds.

Traditional hazard risk assessment approaches are limited since they are primarily based on statistical models which only deal with single meteorological hazards, or use simplified parameterized relationships when more than one phenomenon is included. These statistical modeling approaches also may not adequately reflect risk from future climate changes as they rely entirely upon cyclones statistically generated from the limited observed tropical cyclone record. Dynamical models, on the other hand, promise a complimentary approach that provide a wealth of information on key damaging parameters, but they too suffer from limitations. The most severe of these are coarse horizontal resolution and low sample size. Global Climate Models are also run for all weather conditions; thus, a large fraction of resources is spent on simulations that do not contain severe weather. The HWCM's unique approach fills a gap between statistical and dynamical methods by enabling the generation of dynamical TC simulations that are targeted, detailed, and physically plausible. The ability to focus on specific user-defined multi-hazard TC scenarios means that given the same resources, an order of magnitude more scenarios, at higher resolution, can be created than what is possible with traditional free-running dynamical model simulations. This allows us to not only increase the sample size of the historical event sets used in statistical modeling, but also allows the inclusion of physically plausible events that falls outside the observational record. These dynamical model scenarios may also provide a means of testing and improving statistical approaches for hazard

modeling and informing statistical covariances among the hazards.

This generation of future multi-hazard TC scenarios that fall outside the historical record, but are physically plausible, is a key advantage of this hybrid approach. It also promotes new understanding of the multi-hazards in landfalling TCs and their complex interactions and provides a basis for improving future hazard risk-assessment. Future work will refine model resolution and employ ensembles to improve the quantification of impacts explored here. We will also explore the potential utility of this tool in real world risk decision making environments.

While HWCM was demonstrated here for the case study region of the East Coast of Australia, the approach is globally applicable. Further experiments are needed to determine aspects of the climate change scenarios that are generalizable across TCs and global regions for tropical cyclone impacts in other tropical cyclone basins around the world. For example, while the sign of the change in the areal coverage of strong winds or heavy rainfall may be consistent, the change in the magnitudes or major asymmetries in the change fields may be dependent on characteristics of the TC and its environment.

HWCM may also be used to explore both physically plausible extreme events and the compounding and amplifying effects caused by coincident multi-hazards. Additional model complexity may also be added, depending on the research question or risk assessment need, such as two-way coupling with an ocean model, or coupling to a surge or hydrological model.

Acknowledgements

This material is based upon work supported by the National Center for Atmospheric Research, which is a major facility sponsored by the National Science Foundation under Cooperative Agreement No. 1852977. This work was also supported by the Insurance Australia Group Limited, Sydney, Australia. Computer resources were provided by NCARs' Computational and Information Systems Laboratory. We thank Dr. Andreas Prein for his constructive comments.

Appendix A. Supplementary data

Supplementary data to this article can be found online at https://doi.org/10.1016/j.wace.2019.100229.

References

Vickery, P.J., Skerlj, P., Twisdale, L., 2000. Simulation of hurricane risk in the U.S. using empirical track model. J. Struct. Eng. 10, 1222–1237. https://doi.org/10.1061/(ASCE)07339445(2000)126.

Anthes, R.A., 1982. Tropical cyclones – their evolution, structure, and effects. Meteorol. Monogr. 19 (41). Amer. Meteor. Soc., 208pp.

Bacmeister, J.T., Reed, K.A., Hannay, C., Lawrence, P., Bates, S., Truesdale, J.E., Rosenbloom, N., Levy, M., 2018. Projected changes in tropical cyclone activity under future warming scenarios using a high-resolution climate model. Clim. Change 146 (3–4), 547–560.

BoM, 2018. Tropical Cyclone Debbie Technical Report. Bureau of Meteorology Report. March 2018. http://www.bom.gov.au/cyclone/history/database/Tropical-Cyclone-Debbie-Technical-Report-Final.pdf.

BoM, 2018. Joint Industry Project for Objective Tropical Cyclone Reanalysis: Final Report, p. pp90. September 2018. http://www.bom.gov.au/cyclone/history/database/OTCR-JIP_FinalReport_V1.3_public.pdf.

Borio, C., Drehmann, M., Tsatsaronis, K., 2014. Stress Testing macro stress testing: does it live up to expectations? J. Financ. Stab. 12, 3–15.

Boughton, G., Falck, D., Henderson, D., Smith, D., Parackal, K., Kloetzke, T., Mason, M., Krupar, R., Humphreys, M., Navaratnam, S., Bodhinayake, G., Ingham, I., Ginger, J., 2017. Tropical Cyclone Debbie Damage to Buildings in the Whitsunday Region. TR63, Cyclone Testing Station. James Cook University, Australia.

Bruyère, C.L., CoAuthors, 2017. Impact of Climate Change on Gulf of Mexico Hurricanes. Technical Note NCAR/TN-535+ STR.

Chen, F., Dudhia, J., 2001. Coupling an advanced land-surface/ hydrology model with the Penn State/NCAR MM5 modeling system. Part I: Model implementation and sensitivity. Mon. Wea. Rev. 129, 569–585.

Christensen, J.H., CoAuthors, 2013. Climate phenomena and their relevance for future regional climate change. In: Stocker, T.F., Qin, D., Plattner, G.-K., Tignor, M., Allen, S.K., Boschung, J., Nauels, A., Xia, Y., Bex, V., Midgley, P.M. (Eds.), Climate Change 2013. The Physical Science Basis. Contribution of Working Group I to the Fifth Assessment Report of the Intergovernmental Panel on Climate Change (IPCC AR5). Cambridge University Press, Cambridge, UK and New York, NY.

Cobb, A., Done, J.M., 2017. The use of global climate models for tropical cyclone risk assessment. In: Collins, J.M., Walsh, K. (Eds.), Hurricanes and Climate Change. Springer International Publishing.

CTS, 2018. James Cook University's Cyclone Testing Station has identified a simple and easy to install mitigation initiative could prevent major damage to homes caused by wind-driven water ingress. https://www.iag.com.au/wind-driven-rain-drives-damage-costs.

Czajkowski, J., Done, J.M., 2014. As the wind blows? Developing a deeper understanding of hurricane damages from a case study analysis. Weather Clim. Soc. 6 (2), 202–217. https://doi.org/10.1175/WCAS-D-13-00024.1.

Czajkowski, J., Villarini, G., Montgomery, M., Michel-Kerjan, E., Goska, R., 2017. Assessing current and future freshwater flood risk from North Atlantic tropical cyclones via insurance claims. Sci. Rep. 7, 41609.

Davis, C.A., 2018. Resolving tropical cyclone intensity in models. Geophys. Res. Lett. 45 (4), 2082–2087.

DeMaria, M., Kaplan, J., 1994. A statistical hurricane intensity prediction scheme (SHIPS) for the atlantic basin. Weather Forecast. 9, 209–220. https://doi.org/10.1175/1520-0434(1994)009,0209: ASHIPS.2.0.CO;2.

Done, J.M., Holland, G.J., Bruyère, C.L., Leung, L.R., Suzuki-Parker, A., 2015. Modeling high-impact weather and climate: lessons from a tropical cyclone perspective. Clim. Change 129 (3–4), 381–395.

Done, J.M., Simmons, K.M., Czajkowski, J., 2018. Relationship between residential losses and hurricane winds: role of the Florida building code. ASCE-ASME J. Risk Uncertain. Eng. Syst., Part A: Civ. Eng. 4 (1), 04018001.

Dunion, J.P., 2011. Rewriting the Climatology of the Tropical North Atlantic and Caribbean Sea Atmosphere. J. Clim. 24, 893–907.

Dunion, J.P., Marron, C.S., 2008. A Reexamination of the Jordan Mean Tropical Sounding Based on Awareness of the Saharan Air Layer: Results from 2002. J. Clim. 21, 5242–5253.

Emanuel, K., 1986. An air-sea interaction theory for tropical cyclones. Part I: steady-state maintenance. J. Atmos. Sci. 43, 585–604.

Emanuel, K., 2017. Assessing the present and future probability of Hurricane Harvey's rainfall. Proc. Natl. Acad. Sci. 114, 12681–12684.

Emanuel, K., DesAutels, C., Holloway, C., Korty, R., 2004. Environmental control of tropical cyclone intensity. J. Atmos. Sci. 61, 843–858. https://doi.org/10.1175/1520-0469(2004)061,0843: ECOTCI.2.0.CO;2.

Estrada, F., Botzen, W.W., Tol, R.S., 2015. Economic losses from US hurricanes consistent with an influence from climate change. Nat. Geosci. 8 (11), 880.

Finocchio, P.M., Majumdar, S.J., Nolan, D.S., Iskandarani, M., 2016. Idealized tropical cyclone responses to the height and depth of environmental vertical wind shear. Mon. Weather Rev. 144, 2155–2175. https://doi.org/10.1175/MWR-D-15-0320.1.

Franco, G., Green, R., Khazai, B., Smyth, A., Deodatis, G., 2010. Field damage survey of new orleans homes in the aftermath of hurricane katrina. Nat. Hazards Rev. 11 (1), 7–18.

Gettelman, A., Bresch, D.N., Chen, C.C., Truesdale, J.E., Bacmeister, J.T., 2018. Projections of future tropical cyclone damage with a high-resolution global climate model. Clim. Change 146 (3–4), 575–585.

Gray, W.M., 1968. Global view of the origin of tropical disturbances and storms. Mon. Weather Rev. 96, 669–700.

Grieser, J., Jewson, S., 2012. The RMS TC-rain model. Meteorol. Z. 21 (1), 79–88.

Gurley, K., Masters, F., 2011. Post-2004 hurricane field survey of residential building performance. Nat. Hazards Rev. 12 (4), 177–183.

Gutmann, E.D., Coauthors, 2018. Changes in hurricanes from a 13-yr convection-permitting pseudo – global warming simulation. J. Clim. 31, 3643–3657. https://doi.org/10.1175/JCLI-D-17-0391.1.

Hall, T.M., Jewson, S., 2007. Statistical modelling of North Atlantic tropical cyclone tracks. Tellus 59, 486–498. https://doi.org/10.1111/j.1600-0870.2007.00240.x.

Hall, T.M., Sobel, A.H., 2013. On the impact angle of hurricane Sandy's New Jersey landfall. Geophys. Res. Lett. 40, 2312–2315. https://doi.org/10.1002/grl.50395.

Henderson, D., Ginger, J., 2008. Role of building codes and construction standards in windstorm disaster mitigation. Aust. J. Emerg. Manag. 23/2, 40–46.

Henderson-Sellers, A., Zhang, H., Berz, G., Emanuel, K., Gray, W., Landsea, C., Holland, G., Lighthill, J., Shieh, S.-L., Webster, P., McGuffie, K., 1998. Tropical cyclones and global climate change: a post-IPCC assessment. Bull. Am. Meteorol. Soc. 79, 19–38.

Holland, G.J., 1983. Tropical cyclone motion: environmental interaction plus a beta effect. J. Atmos. Sci. 40, 328–342.

Holland, G.J., Bruyère, C.L., 2014. Recent intense hurricane response to global climate change. Clim. Dyn. 42, 617. https://doi.org/10.1007/s00382-013-1713-0.

Holland, G.J., Belanger, J.I., Fritz, A., 2010. A revised model for radial profiles of hurricane winds. Mon. Weather Rev. 138, 4393–4401.

Hong, S.-Y., Dudhia, J., Chen, S.-H., 2004. A revised approach to ice-microphysical processes for the bulk parameterization of cloud and precipitation. Mon. Wea. Rev. 132, 103–120.

Hong, S.-Y., Noh, Y., Dudhia, J., 2006. A new vertical diffusion package with an explicit treatment of entrainment processes. Mon. Wea. Rev. 134, 2318–2341. https://doi.org/10.1175/MWR3199.1.

Huang, X.-Y., Yang, X., 2002. A new implementation initialization of digital filtering schemes for HIRLAM. HIRLAM Tech. Rep. 53, 36 pp.

Kaplan, J., DeMaria, M., 2003. Large-scale characteristics of rapidly intensifying tropical cyclones in the North At- lantic basin. Weather Forecast. 18, 1093–1108. https://doi.org/10.1175/1520-0434(2003)018,1093:LCORIT.2.0.CO;2.

Kimball, S.K., 2008. Structure and evolution of rainfall in numerically simulated landfalling hurricanes. Mon. Weather Rev. 136, 3822–3847.

Knutson, T.R., Tuleya, R.E., Kurihara, Y., 1998. Simulated increase of hurricane intensities in a CO2-warmed climate. Science 279, 1018–1020.
Knutson, T.R., et al., 2010. Tropical cyclones and climate change. Nat. Geosci. 3, 157–163.
Knutson, T.R., Sirutis, J.J., Zhao, M., Tuleya, R.E., Bender, M., Vecchi, G.A., Villarini, G., Chavas, D., 2015. Global projections of intense tropical cyclone activity for the late twenty-first century from dynamical downscaling of CMIP5/RCP4.5 scenarios. J. Clim. 28, 7203–7224.
Kossin, J.P., Emanuel, K.A., Vecchi, G.A., 2014. The poleward migration of the location of tropical cyclone maximum intensity. Nature 509 (7500), 349–352.
Kuleshov, Y.R., Fawcett, R., Qi, L., Trewin, B., Jones, D., McBride, J., Ramsay, H., 2010. Trends in tropical cyclones in the south Indian ocean and the south Pacific Ocean. J. Geophys. Res. Atmos. 115, D01101.
Landsea, C.W., Franklin, J.L., 2013. Atlantic hurricane database uncertainty and presentation of a new database format. Mon. Weather Rev. 141, 3576–3592.
Langousis, A., Veneziano, D., 2009. Long-term rainfall risk from tropical cyclones in coastal areas. Water Resour. Res. 45 (W11430) https://doi.org/10.1029/2008WR007624.
Lavender, S.L., Walsh, K.J.E., 2011. Dynamically downscaled simulations of Australian region tropical cyclones in current and future climates. Geophys. Res. Lett. 38. L10705.
Lavender, S.L., Hoeke, R.K., Abbs, D.J., 2018. The influence of sea surface temperature on the intensity and associated storm surge of tropical cyclone Yasi: a sensitivity study. Nat. Hazards Earth Syst. Sci. 18, 795–805.
Lee, C.Y., Tippett, M.K., Sobel, A.H., Camargo, S.J., 2018. An environmentally forced tropical cyclone hazard model. J. Adv. Model. Earth Syst. 10, 223–241. https://doi.org/10.1002/2017MS001186.
Li, Y., Cheunga, K.K.W., Chan, J.C.L., 2015. Modelling the effects of land–sea contrast on tropical cyclone precipitation under environmental vertical wind shear. Q. J. R. Meteorol. Soc. 141, 396–412. https://doi.org/10.1002/qj.2359.
Lighthill, J., Zheng, Z., Holland, G.J., Emanuel, K. (Eds.), 1993. Tropical Cyclone Disasters. Peking University Press, Beijing, 7-301-02086-4/P.31, 588 pp.
Lin, N., Emanuel, K.A., Smith, J.A., Vanmarcke, E., 2010. Risk assessment of hurricane storm surge for New York City. J. Geophys. Res. B 115. https://doi.org/10.1029/2009JD013630. D18121.
Lin, N.K., 2016. Grey swan tropical cyclones. Nat. Clim. Change 6, 106–111.
Lin, N., Emanuel, K.A., Oppenheimer, M., Vanmarcke, E., 2012. Physically based assessment of hurricane surge threat under climate change. Nat. Clim. Chang. 2 (6), 462–467.
Lindzen, R.S., Nigam, S., 1987. On the role of seas surface temperature gradients on forcing low-level winds and convergence in the tropics. J. Atmos. Sci. 44, 2418–2436.
Lonfat, M., Rogers, R., Marchok, T., Marks Jr., F.D., 2007. A parametric model for predicting hurricane rainfall. Mon. Weather Rev. 135 (9) https://doi.org/10.1175/MWR3433.1.
Loridan, T., Mason, M.S., 2017. Using Realistic Disaster Scenario Analysis to Understand Natural Hazard Impacts and Emergency Management Requirements: Annual Project Report 2016-17. Bushfire and Natural Hazards CRC.
Merrill, R.T., 1988. Environmental influences on hurricane intensification. J. Atmos. Sci. 45, 1678–1687.
Milly, P.C.D., Betancourt, J., Falkenmark, M., Hirsch, R.M., Kundzewicz, Z.W., Lettenmaier, D.P., Stouffer, R.J., 2008. Stationarity is dead: whither water management? Science 319, 573–574. https://doi.org/10.1126/science.1151915.
Mlawer, E.J., Taubman, S.J., Brown, P.D., Iacono, M.J., Clough, S.A., 1997. Radiative transfer for inhomogeneous atmospheres: RRTM, a validated correlated-k model for the longwave. J. Geophys. Res. 102D, 16663–16682.
Morss, R.E., Wilhelmi, O.V., Meehl, G.A., Dilling, L., 2011. Improving societal outcomes of extreme weather in a changing climate: an integrated perspective. Annu. Rev. Environ. Resour. 36, 1–25. https://doi.org/10.1146/annurev-environ-060809-100145.
Munich Re, 2018. Topics Geo: natural catastrophes 2017. Analyses, assessments, positions. Available at: www.munichre.com/topicsgeo2017.
Murnane, R.J., Elsner, J.B., 2012. Maximum wind speeds and US hurricane losses. Geophys. Res. Lett. 39 (16).
Nerem, R.S., Beckley, B.D., Fasullo, J.T., Hamlington, B.D., Masters, D., Mitchum, G.T., 2018. Climate-change– driven accelerated sea-level rise detected in the altimeter era. Proc. Natl. Acad. Sci. 201717312.
Onderlinde, M.J., Nolan, D.S., 2014. Environmental helicity and its effects on development and intensification of tropical cyclones. J. Atmos. Sci. 71, 4308–4320. https://doi.org/10.1175/JAS-D-14-0085.1.
Palmén, E.H., 1948. On the formation and structure of tropical cyclones. Geophysica 3, 26–38. Helsinki.
Parker, C.L., Bruyère, C.L., Mooney, P.A., Lynch, A.H., 2018. The response of land-falling tropical cyclone characteristics to projected climate change in northeast Australia. Clim. Dyn. https://doi.org/10.1007/s00382-018-4091-9.
Risser, M.D., Wehner, M.F., 2017. Attributable human-induced changes in the likelihood and magnitude of the observed extreme precipitation during hurricane Harvey. Geophys. Res. Lett. 44 (24).
Rotunno, R., Chen, Y., Wang, W., Davis, C., Dudhia, J., Holland, G.J., 2009. Large-eddy simulation of an idealized tropical cyclone. Bull. Am. Meteorol. Soc. 90, 1783–1788.
Rumpf, J., Weindl, H., Höppe, P., et al., 2007. Stochastic modelling of tropical cyclone tracks. Math. Methods Oper. Res. 66, 475–490. https://doi.org/10.1007/s00186-007-0168-7.
Shaevitz, D.A., et al., 2014. Characteristics of tropical cyclones in high-resolution models in the present climate. J. Adv. Model. Earth Syst. 6 (4), 1154–1172.
Skamarock, W., CoAuthors, 2008. A description of the advanced research WRF version 3. NCAR Tech. Note 475, 113 pp.
Climate change 2007: the physical science basis. In: Solomon, S., et al. (Eds.), 2007. Contribution of Working Group I to the Fourth Assessment Report of the IPCC, vol. 4. Cambridge University Press, Cambridge, United Kingdom and New York, NY, USA.
Sumi, A., 1992. Pattern formation of convective activity over the aqua-planet with globally uniform sea surface temperature (SST). J. Met. Soc. Jpn. 70, 855–876.
Tang, B., Emanuel, K., 2012. Sensitivity of tropical cyclone intensity to ventilation in an axisymmetric model. J. Atmos. Sci. 69, 2394–2413.
Trenberth, K.E., Cheng, L., Jacobs, P., Zhang, Y., Fasullo, J., 2018. Hurricane Harvey links to ocean heat content and climate change adaptation. Earth's Future. https://doi.org/10.1029/2018EF000825.
Tuleya, R.E., Kurihara, Y., 1978. A numerical simulation of the land- fall of tropical cyclones. J. Atmos. Sci. 35, 242–257.
Tuleya, R.E., Bender, M.A., Kurihara, Y., 1984. A simulation study of the landfall of tropical cyclones. Mon. Weather Rev. 112, 124–136.
Vickery, P.J., 2005. Simple empirical models for estimating the increase in the central pressure of tropical cyclones after landfall along the coastline of the United States. J. Appl. Meteorol. 44 (12), 1807–1826.
Villarini, G., Lavers, D.A., Scoccimarro, E., Zhao, M., Wehner, M.F., Vecchi, G.A., Knutson, T.R., Reed, K.A., 2014. Sensitivity of tropical cyclone rainfall to idealized global-scale forcings. J. Clim. 27, 4622–4641. https://doi.org/10.1175/JCLI-D-13-00780.
Vitolo, R., Strachan, J., Vidale, P.L., Stephenson, D., Cook, I., Flay, S., Foote, M., 2010. A Global Climate Model based event set for tropical cyclone risk assessment in the West Pacific. In: Abstracts from EGU General Assembly, Vienna, Austria, 2-7 May 2010.
Wakimoto, R.M., Black, P.G., 1994. Damage survey of Hurricane Andrew and its relationship to the eyewall. Bull. Amer. Met. Soc. 75, 189–200.
Walsh, K.J.E., McBride, J.L., Klotzbach, P.J., Balachandran, S., Camargo, S.J., Holland, G.J., Knutson, T.R., Kossin, J.P., Lee, T.-C., Sobel, A., Sugi, M., 2016. Tropical cyclones and climate change. WIREs Clim. Chang. 7, 65–89. https://doi.org/10.1002/wcc371.
Weinkle, J., Maue, R., Pielke Jr., R., 2012. Historical global tropical cyclone landfalls. J. Clim. 25 (13), 4729–4735.
Weygandt, S.S., Benjamin, S., 2007. Radar reflectivity-based initialization of precipitation systems using a diabatic digital filter within the Rapid Update Cycle. In: 22nd Conf. On Weather Analysis and Forecasting/18th Conf. on Numerical Weather Prediction, Park City, UT, Amer. Meteor. Soc., 1B.7. https://ams.confex.com/ams/22WAF18NWP/techprogram/paper_124540.htm.
Willoughby, H., Darling, R., Rahn, M., 2006. Parametric representation of the primary hurricane vortex. part II: a new family of sectionally continuous profiles. Mon. Weather Rev. 134 (4), 1102–1120.
Zhao, M., Held, I.M., Vecchi, G., Scoccimarro, E., Wang, H., Wehner, M., Lim, Y.-K., LaRow, T., Camargo, S.J., Walsh, K., et al., 2013. Robust direct effect of increasing atmospheric CO2 concentration on global tropical cyclone frequency—a multi-model inter-comparison. CLIVAR Var. 11, 17–23.